

## Ultrathin Polymer Film Formation by Collision-Induced Cross-Linking of Adsorbed Organic Molecules with Hyperthermal Protons

Zhi Zheng,<sup>†</sup> Xiangdong Xu,<sup>†</sup> Xiaoli Fan,<sup>‡</sup> Woon Ming Lau,<sup>‡</sup> and Raymund Wai Man Kwok<sup>\*†</sup>

*Contribution from the Departments of Chemistry and of Physics and Materials Science and Technology Research Centre, The Chinese University of Hong Kong, Shatin, Hong Kong, People's Republic of China*

Received May 28, 2004; E-mail: rmkwok@cuhk.edu.hk

**Abstract:** A new synthetic approach for the formation of ultrathin polymer films with customizable properties was developed. In this approach, the kinematic nature of proton collisions with simple organic molecules condensed on a substrate is exploited to break C–H bonds preferentially. The subsequent recombination of carbon radicals gives a cross-linked polymer thin film, and the selectivity of C–H cleavage preserves the chemical functionalities of the precursor molecules. The nature and validity of the method are exemplified with theoretical results from ab initio molecular dynamics calculations and experimental evidence from a variety of characterization techniques. Its applicability is demonstrated by the synthesis of ultrathin polymer films with precursor molecules such as dotriacontane, docosanoic acid, poly(acrylic acid) oligomer, and polyisoprene. The approach is fundamentally different from conventional chemical synthesis as it involves an unusual mix of physical and chemical processes including charge exchange, projectile penetration, kinematics, collision-induced dissociation, inelastic energy transfer, chain transfer, and chain cross-linking.

### Introduction

The momentum and kinetic energy of a reactant are rarely considered as design parameters by synthetic chemists, despite that these factors are critical in many practical materials processes employing physical sputtering for surface cleaning, reactive ion etching for submicrometer device fabrication, ion implantation for semiconductor doping, and ion-assisted film deposition. For enriching our understanding of the underlying science, Ceyer<sup>1</sup> vividly used “chemistry with a hammer” to illustrate some unusual features of this reaction design. She employed hyperthermal<sup>2</sup> Kr as the “hammer” to dissociate CH<sub>4</sub> on Ni(111), and showed that the whole molecule is excited due to the large collision cross-section of the hammer. In comparison, when the Kr energy is raised to 10 keV, the collision cross-section shrinks and the projectile becomes a “bullet” which can recoil<sup>2</sup> a single constituent atom of a target, like “chemistry with a bullet”. Although these hammer and bullet promote chemical reactivity, they are not chemically selective. Here, we show that, when hyperthermal protons collide with adsorbed organic molecules, C–H bonds can be preferentially cleaved with the preservation of other bonds. The subsequent recom-

bination of carbon radicals can be exploited to produce novel polymeric films with tailor-made chemical functionalities. More importantly, the reactivity and chemical selectivity of these unusual reactions display intriguing effects and applicability of kinematics and inelastic collision in the design of chemical reactions.

Unlike photon and electron irradiation which can promote reactivity with chemical selectivity through their direct coupling to the electronic structures of the reactants, the reaction driving forces of atom/molecule projectiles are more complex and typically influenced by charge exchange and translation–potential (T–V) energy conversion among all parties in the collision events induced by the entry of the projectile into the reaction system.<sup>1–8</sup> Typically, projectile chemistry and energy are the key reaction attributes for improving chemical selectivity and reactivity in the design of collision-induced chemistry. The recent successes in controlled soft-landing<sup>4,5</sup> of hyperthermal polyatomic molecules or molecular ions fully exploit the projectile chemistry in the yield of reaction products with specific chemical functionalities. However, the industrial ap-

<sup>†</sup> Department of Chemistry and Materials Science and Technology Research Centre.

<sup>‡</sup> Department of Physics and Materials Science and Technology Research Centre.

(1) Ceyer, S. T. *Science* **1990**, *249*, 133–139.

(2) Hyperthermal energy is typically referred to the regime of 1–100 eV. See, for example: Jacobs, D. C. Reactive collisions of hyperthermal energy molecular ions with solid surfaces. *Annu. Rev. Phys. Chem.* **2002**, *53*, 379–407.

(3) (a) Rabalais, J. W. *CRC Crit. Rev. Solid State* **1988**, *14*, 319–376. (b) Rabalais, J. W. *Science* **1990**, *250*, 521–527.

(4) Miller, S. A.; Luo, H.; Pachuta, S. J.; Cooks, R. G. *Science* **1997**, *275*, 1447–1450.

(5) Ouyang, Z.; Takats, Z.; Blake, T. A.; Gologan, B.; Guymon, A. J.; Wiseman, J. M.; Oliver, J. C.; Davisson, V. J.; Cooks, R. G. *Science* **2003**, *301*, 1351–1354.

(6) Kasi, S. R.; Kang, H.; Sass, C. S.; Rabalais, J. W. *Surf. Sci. Rep.* **1989**, *10*, 1–104.

(7) Lau, W. M.; Kwok, R. W. M. *Int. J. Mass Spectrom. Ion Processes* **1998**, *174*, 245–252.

(8) Kleyn, A. W. *Chem. Soc. Rev.* **2003**, *32*, 87–95.

plicability of soft-landing molecular species is inevitably confined by the cost-effectiveness in production and delivery of the required molecular species in a large area.

To design an alternative practical route for improving chemical selectivity in chemistry with a hammer, we focus our attention to effective T–V conversion. Particularly, we consider that under the simple hard-sphere binary collision model<sup>9</sup> an atomic hydrogen projectile at 10 eV can at the most transfer 2.8 eV to a carbon atom of the hydrocarbon framework of an organic molecule through a head-on collision of the two atoms, while the energy transfer to a hydrogen atom of the organic molecule can reach 10 eV. Since the typical bond energy for a single bond such as C–H and C–C is about 3–5 eV in common organic molecules, conceivably collision with atomic hydrogen projectiles at 10 eV can cleave C–H bonds and may leave all C–Z bonds intact, where Z is any common constituent atom heavier than hydrogen. With this chemical selectivity by kinematics, we can select certain precursor molecules, condense them on a substrate surface, cleave some C–H bonds, and let the activated molecules cross-link to a polymeric film with tailor-made chemical functionalities of the precursor molecules.

It is relevant to compare the proposed collision approach with simple hydrogen abstraction,<sup>10</sup> a thermally driven reaction in which a hydrogen atom breaks a C–H bond in a hydrocarbon molecule to form a hydrogen molecule and a hydrocarbon molecule with a carbon radical. This reaction is almost enthalpy neutral or slightly exothermal, with a small energy barrier<sup>11</sup> of about 0.4 eV. Hence, it can proceed even at room temperature. Nevertheless, our proposed collision approach with hyperthermal hydrogen projectiles offers two advantages over simple hydrogen abstraction. First, the reactivity leading to C–H cleavage increases drastically from  $\sim 0.05 \text{ \AA}^2$  for the hydrogen atom (in an Eley–Rideal-type reaction) at 300–400 K ( $\sim 0.04 \text{ eV}$ )<sup>10</sup> to  $1.2 \text{ \AA}^2$  at 0.7 eV and  $1.5 \text{ \AA}^2$  at 1.6 eV.<sup>12</sup> It is thus reasonable to expect a 100-fold increase of reactivity by optimizing the reaction with projectile energy. Second, the collision approach promotes projectile penetration and mobility below the surface of a film of adsorbed or condensed hydrocarbon molecules, which is indeed exploited in this work to produce novel polymeric films. It is known experimentally<sup>13</sup> that argon at 15 eV can penetrate to  $10 \text{ \AA}$  in a silicon crystal. A recent computer simulation<sup>14</sup> also shows that  $\text{H}^+$  at 10 eV can go as deep as  $\sim 10 \text{ \AA}$  in an amorphous hydrogen-containing carbon film.

The proposed reaction design relies on a seemingly oversimplified binary collision for chemical selectivity. However, the design is not ungrounded because Tongson and Cooper<sup>15</sup> indeed found that 20 eV  $\text{Ne}^+$  colliding with copper follows the kinematics of hard-sphere binary scattering. On the other hand, previous experimental studies<sup>16–18</sup> of  $\text{H}^+$  collision with gaseous  $\text{CH}_4$ ,  $\text{C}_2\text{H}_2$ , and  $\text{C}_2\text{H}_4$  in the energy range of 10–30 eV showed

that the projectile can transfer energy to its collision partner via mechanisms including (a) vibration excitation of the target molecule through its long-range dipole coupling with the moving proton, (b) charge exchange, and (c) internal energy transfer through a quasi-molecule transition state in close encounter. In short, in our proposed reaction design, reactivity and chemical selectivity will be affected by both the physical kinematics and these inelastic factors in the reaction. In this context, it is relevant to note that several researchers active in plasma-assisted deposition<sup>10,19,20</sup> and etching of hydrocarbon films<sup>10,20–22</sup> have also recognized and confirmed the importance of the individual and synergetic effects of such physical and chemical factors in their reaction systems. In particular, von Keudell, Jacob, and their co-workers<sup>23</sup> have recently articulated the collision nature that hydrogen ions impinging on a hydrocarbon film can penetrate into the film and preferentially displace its hydrogen atoms. This was exploited to engineer the extent of cross-linking, film density, and hydrogen content of the resultant hydrocarbon film.

## Results and Discussion

**Computational Analysis.** To further assess the validity and feasibility of our reaction design, we performed quantum chemistry calculations<sup>24</sup> of the reaction dynamics in a sequence of 0.05 fs steps for 50 selective collision configurations most likely leading to C–H and C–C bond cleavages in the collision systems including (a) a proton ( $\text{H}^+$ ) hitting a simple hydrocarbon,  $\text{H}^+ \rightarrow n\text{-C}_x\text{H}_{2x+2}$ , and (b) a hydrogen atom (H) hitting a simple hydrocarbon:  $\text{H} \rightarrow n\text{-C}_x\text{H}_{2x+2}$ , for  $x$  up to 6 as a function of projectile energy. For the simulation of each collision configuration, we initiated it by setting the initial velocity and orientation of the projectile relative to the target molecule. The electronic energies and forces were calculated with the quantum chemistry code. The velocities and orientations of the atoms were updated for the next time step, and the iteration continued until the end of the collision event, which typically lasted for about 100 fs.

In our sampling of collision configurations, we found that, with an impact energy of 10 eV, a H projectile can cleave C–H but no C–C bond for all calculated molecules. Although the results support our proposed preferential C–H cleavage, the details in collision dynamics deviate significantly from the kinematics of binary atomic collision. In brief, some kinetic energy of the projectile is being transferred to the molecular

- (9) Parilis, E. S. *Atomic collisions on solid surfaces*; North-Holland Press: Amsterdam, 1993; pp 21–24.
- (10) Küppers, J. *Surf. Sci. Rep.* **1995**, *22*, 251–321.
- (11) Zavitsas, A. A. *J. Am. Chem. Soc.* **1998**, *120*, 6578–6586.
- (12) Germann, G. J.; Huh, Y. D.; Valentini, J. J. *J. Chem. Phys.* **1992**, *96*, 5746–5757.
- (13) Lau, W. M.; Bello, I.; Huang, L. J.; Feng, X.; Vos, M.; Mitchell, I. V. *J. Appl. Phys.* **1993**, *74*, 7101–7106.
- (14) Salonen, E.; Nordlund, K.; Keinonen, J.; Wu, C. H. *Phys. Rev. B* **2001**, *63*, 195415, 1–14.
- (15) Tongson, L. L.; Cooper, C. B. *Surf. Sci.* **1975**, *52*, 263–269.
- (16) Chiu, Y.-N.; Friedrich, B.; Maring, W.; Niedner, G.; Noll, M.; Toennies, J. P. *J. Chem. Phys.* **1988**, *88*, 6814–6830.
- (17) Aristov, N.; Niederschattberg, G.; Toennies, J. P.; Chiu, Y. N. *J. Chem. Phys.* **1991**, *95*, 7969–7983.

- (18) Aristov, N.; Maring, W.; Niederschattberg, G.; Toennies, J. P.; Chiu, Y. N.; Koppel, H. *J. Chem. Phys.* **1993**, *99*, 2682–2694.
- (19) von Keudell, A. *Nucl. Instrum. Methods, B* **1997**, *125*, 323–327.
- (20) Jacob, W. *Thin Solid Films* **1998**, *326*, 1–42.
- (21) Annen, A.; Jacob, W. *Appl. Phys. Lett.* **1997**, *71*, 1326–1328.
- (22) Hopf, C.; von Keudell, A.; Jacob, W. *J. Appl. Phys.* **2003**, *94*, 2373–2380.
- (23) Hopf, C.; von Keudell, A.; Jacob, W. *Diamond Relat. Mater.* **2003**, *12*, 85–89.
- (24) Frisch, M. J.; Trucks, G. W.; Schlegel, H. B.; Scuseria, G. E.; Robb, M. A.; Cheeseman, J. R.; Zakrzewski, V. G.; Montgomery, J. A.; Stratmann, R. E.; Burant, J. C.; Dapprich, S.; Millam, J. M.; Daniels, A. D.; Kudin, K. N.; Strain, M. C.; Farkas, O. Tomasi, J.; Barone, V.; Cossi, M.; Cammi, R.; Mennucci, B.; Pomelli, C.; Adamo, C.; Clifford, S.; Ochterski, J.; Petersson, G. A.; Ayala, P. Y.; Cui, Q.; Morokuma, K.; Salvador, P.; Dannenberg, J. J.; Malick, D. K.; Rabuck, A. D.; Raghavachari, K.; Foresman, J. B.; Cioslowski, J.; Ortiz, J. V.; Baboul, A. G.; Stefanov, B. B.; Liu, G.; Liashenko, A.; Piskorz, P.; Komaromi, I.; Gomperts, R.; Martin, R. L.; Fox, D. J.; Keith, T.; Al-Laham, M. A.; Peng, C. Y.; Nanayakkara, A.; Challacombe, M.; Gill, P. M. W.; Johnson, B.; Chen, W.; Wong, M. W.; Andres, J. L.; Gonzalez, C.; Head-Gordon, M.; Replogle, E. S.; and Pople, J. A. *Gaussian 98, G98A*, 11th ed.; Gaussian, Inc.: Pittsburgh, PA, 2001.

constituents of the target as both kinetic energy and internal energy. Nevertheless, for the same target molecule, energy transfer from the H projectile to the collided molecule is still more efficient for collisions hitting a hydrogen atom of the molecule than those hitting a carbon atom. For collisions with a 10 eV H projectile, the kinetic energy loss of the projectile head-on colliding with a hydrogen atom of the target molecule ranges from  $\sim 3$  to 7 eV, depending on the spatial collision configuration. Although the maximum energy transfer is less than that predicted by the binary collision model (10 eV), it is still sufficient to induce collisional cleavage of C–H bonds in the target molecule. In comparison, our data show that a H projectile head-on colliding with a carbon atom has a smaller kinetic energy loss of  $\sim 2$ –3 eV, and this energy transfer is not sufficient for collision-induced C–C bond cleavage. In short, the calculations of molecular dynamics using simple hydrocarbons support our proposed collision approach in reaction design and enrich its theoretical framework beyond the oversimplified binary atomic collision model.

Although a hyperthermal  $H^+$  projectile will likely be neutralized when it is close to the surface of the substrate because its empty 1s state lies in the valence band of the substrate and is far below its Fermi level, the study of molecular dynamics in the context of the present work is not complete without the consideration of collisions with  $H^+$ . In comparison to a H projectile, a  $H^+$  projectile behaves differently in that the exothermal charge transfer from the projectile to a hydrocarbon molecule, which typically supplies an energy of  $\sim 3$  eV, eases C–H and C–C cleavage. Our calculations show that, while a 10 eV  $H^+$  arriving along the C–C axis still cannot cleave the C–C bond, it can cleave C–C by approaching a carbon atom perpendicularly to the C–C axis in some collision configurations. These situations of C–C cleavage can, however, be prevented by reducing the kinetic energy of the  $H^+$  projectile. Overall, the calculation results for collisions with hyperthermal  $H^+$  illustrate qualitatively the possible impacts of charge transfer in both chemical reactivity and selectivity.

Our calculation results are consistent with those of Salonen et al.,<sup>14</sup> who gave a very small carbon sputtering yield of  $\sim 0.01$  for 10 eV  $H^+$  hitting a hydrogenated carbon film, together with a much higher probability of removing hydrogen from the film. Further, they found that increasing the projectile mass from  $H^+$  to  $D^+$  alone raised the carbon sputtering yield to  $\sim 0.02$ . Hence, kinematics is indeed relevant.

**Experimental Studies.** To test our reaction design experimentally, we selected dotriacontane,  $CH_3(CH_2)_{30}CH_3$ , as a precursor molecule and used a beam of  $10 \pm 0.6$  eV  $H^+$  to cleave C–H bonds in a vacuum and cross-link the simple saturated hydrocarbon chains into a polymeric film. The trial was then extended as a function of projectile energy in the range of 3–150 eV. Dotriacontane was selected because the molecule is large enough that it does not desorb in a vacuum at room temperature, and yet it is small enough that its solubility in benzene allows its uniform deposition on a convenient substrate such as a silicon wafer by spin-casting. The film thickness was typically about 5–12 nm in this work. Atomic force microscopy (AFM) was employed to confirm the film uniformity and changes in relative mechanical strength induced by cross-linking. In situ X-ray photoelectron spectroscopy (XPS) verified the presence of no elements but carbon on the atomically clean

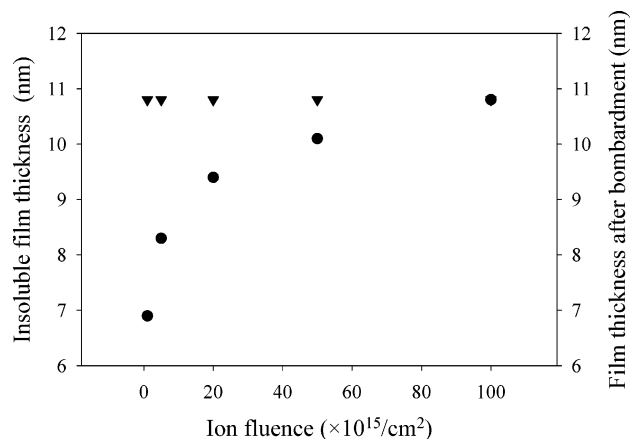


**Figure 1.** Extents of cross-linking (insoluble film thickness after solvent immersion, denoted as circles) and C–C cleavage (film thickness before solvent immersion, denoted as triangles) as a function of ion fluence with 10 eV  $H^+$  ion bombardment of an 11 nm dotriacontane film.

H-terminated silicon surface, which supports the purity and stability of the deposited dotriacontane molecules. XPS was also used to measure film thickness. In addition, characteristic electron energy loss spectroscopy (EELS) was employed to confirm the absence of any unsaturated carbon bonds in all spin-cast films and bombarded films. The results indicate that there was no residual solvent (benzene) in the film and unsaturated bonds were not formed by the collision.

Several pieces of experimental evidence demonstrate consistently the feasibility of cross-linking dotriacontane by 10 eV  $H^+$  collision.

First, the as-deposited dotriacontane molecules can be washed off with a solvent such as hexane, dissolution which was confirmed by XPS film thickness measurements. Such dissolution became incomplete after the dotriacontane film was treated by 10 eV  $H^+$  collision, as shown in Figure 1. For a dotriacontane film with an original thickness of 11 nm, a total ion fluence of  $2 \times 10^{16}/\text{cm}^2$  led to the formation of an insoluble film with a residual thickness of  $\sim 9$  nm after the dissolution test. This thickness is equivalent to the presence of  $\sim 1 \times 10^{15}$  dotriacontane molecules/ $\text{cm}^2$ . Hence, on the average, 10–20  $H^+$  projectiles at 10 eV were sufficient to cross-link one dotriacontane molecule into a polymeric network large enough to resist dissolution by organic solvents. While this analysis illustrates the high reaction effectiveness of the collision-induced C–H cleavage and subsequent cross-linking, the experimental result that continuous bombardment to ion fluence over  $10^{17}/\text{cm}^2$  did not induce any noticeable film thickness reduction (Figure 1) confirms the negligible probability of C–C cleavage.

The second piece of experimental evidence of cross-linking of dotriacontane molecules by 10 eV  $H^+$  collision is shown in Figure 2, which displays the changes of the valence band spectrum of an 11 nm dotriacontane film as a function of ion fluence. The two spectral peaks of the virgin film at 14 and 19 eV are characteristics of the C 2s valence electrons of hydrocarbon chains with no branching. Similar spectral features are found from polyethylene, as shown in the inset in Figure 2, except some peak broadening associated with the chain length difference between dotriacontane and polyethylene. In comparison, polypropylene possesses  $-CH_3$  side branches, and this gives a distinct peak at  $\sim 17$  eV (inset in Figure 2). Hence, the observed emergence of spectral signals at  $\sim 17$  eV in conjunction



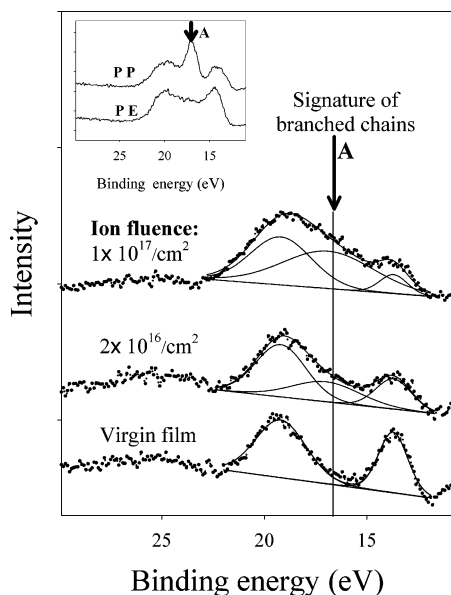


**Figure 2.** XPS valence band spectra of the virgin and 10 eV  $H^+$  ion beam treated dotriacontane films. Inset: valence band spectra of polyethylene (PE) and polypropylene (PP).

with  $H^+$  collisions of dotriacontane molecules (Figure 2) gives clear spectral evidence of cross-linking and side-branch formation. In addition to this change, the spectral band at 14 eV dropped in intensity with increasing ion fluence. To explain this, we adopt the quantum chemistry calculations of Deleuze and Delhalle,<sup>25</sup> who showed that, when a saturated hydrocarbon is cross-linked into a rigid cage such as adamantane, the induced bond strain correlates with the intermixing of the C 2s band (above 14 eV) with the “C 2p–H 1s” band (below 10 eV). The latter band has a relatively weak photoemission cross-section so that the observed spectral intensity reduction at the low end of the valence band in Figure 2 can be an indication of extensive cross-linking and associated strain in the resultant three-dimensional network. A similar spectral intensity change was indeed also observed when the strain was altered in polyethylene.<sup>26</sup>

In addition, we have also confirmed cross-linking of dotriacontane molecules by static secondary ion mass spectrometry (SIMS). Conceptually, SIMS is an effective means to detect any increase in branching or cross-linking of an aliphatic polymer because branching/cross-linking leads to the formation of additional tertiary carbon sites and SIMS signals of large fragment ions are enriched when they contain tertiary carbon sites which stabilize the positive charge of the fragment ion. In practice, SIMS signals of the fragments  $C_nH_{2x+1}^+$  with  $n \geq 6$  and  $x \leq n$  have been found to be sensitive to changes in branching/cross-linking. Upon this platform, van Ooij and Brinkhuis<sup>27</sup> proposed to use the intensity ratio of the most intense fragment ion for  $n = 8$  to the most intense fragment ion for  $n = 2$ . Subsequently Lianos et al.<sup>28</sup> showed that the ratio of the sum of  $C_nH_{2x+1}^+$  for  $n = 6-8$  to the sum of  $C_nH_{2x+1}^+$  for  $n = 2-8$  is statistically more reliable as an indicator of the degree of branching/cross-linking in an aliphatic

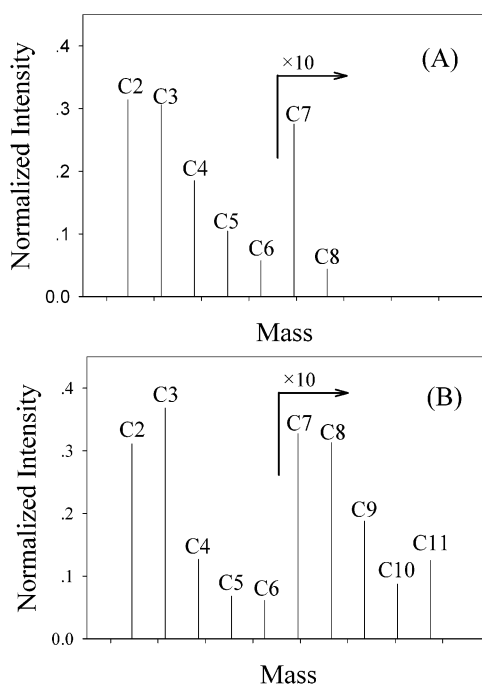


**Figure 3.** Positive static secondary ion mass spectra of (A) an original dotriacontane film and (B) a 10 eV  $H^+$  treated film at a dose of  $2 \times 10^{16}/\text{cm}^2$ . Each peak labeled as  $C_n$  in the bar graph shows the sum of all signals of the  $C_nH_{2x+1}$  clusters.

polymer. In the present study, we adopted these SIMS techniques and compared the mass spectra (Figure 3) of the virgin film and bombarded film. The result clearly shows the increases in the normalized intensity for fragment ions having more than seven carbon atoms as a consequence of the film treatment with 10 eV  $H^+$ . Following the model of Lianos et al.<sup>28</sup> for deducing the degree of branching and cross-linking in saturated hydrocarbon polymers, we calculated the intensity ratio of the fragments with 6–8 carbons to that with 2–8 carbons and found that the ratio increased from  $\sim 9\%$  for the virgin dotriacontane film to  $\sim 13\%$  for the treated film. In comparison, Lianos et al.<sup>28</sup> found a ratio of  $\sim 7-9\%$  for polyethylene and 9–14% for polypropylene. Therefore, our SIMS analysis indeed shows a strong correlation between cross-linking of organic precursor molecules and 10 eV  $H^+$  bombardment of the film containing these molecules.

The fourth piece of evidence of cross-linking of a dotriacontane film comes from contact mode AFM studies. With the same force conditions for AFM imaging, the AFM scans of the virgin film show the development of film holes torn by the AFM tip (Figure 4a), mechanical deficiencies which were not found after the film was treated by 10 eV  $H^+$  with an ion fluence above  $10^{15}/\text{cm}^2$  (Figure 4b). Although qualitative in nature, the observed increase in mechanical strength of the treated film is consistent with the cross-linking of dotriacontane into a comparatively rigid hydrocarbon network. The production of coherent films with mechanical strength is indeed an attractive feature of our reaction design.

The projectile incident energy is a critical design parameter in this work, and this is revealed by the film thickness data collected with a constant ion fluence of  $2 \times 10^{16}/\text{cm}^2$  as a function of energy (Figure 5). The film thickness reduction induced by  $H^+$  bombardment was measured immediately after

(25) Deleuze, M.; Delhalle, J. *Int. J. Quantum Chem.* **1996**, *60*, 293–302.

(26) Galuska, A. A.; Halverson, D. E. *Surf. Interface Anal.* **1998**, *26*, 425–432.

(27) van Ooij, W. J.; Brinkhuis, R. H. G. *Surf. Interface Anal.* **1988**, *11*, 430–440.

(28) Lianos, L.; Quet, C.; Duc, T. M. *Surf. Interface Anal.* **1994**, *21*, 14–22.

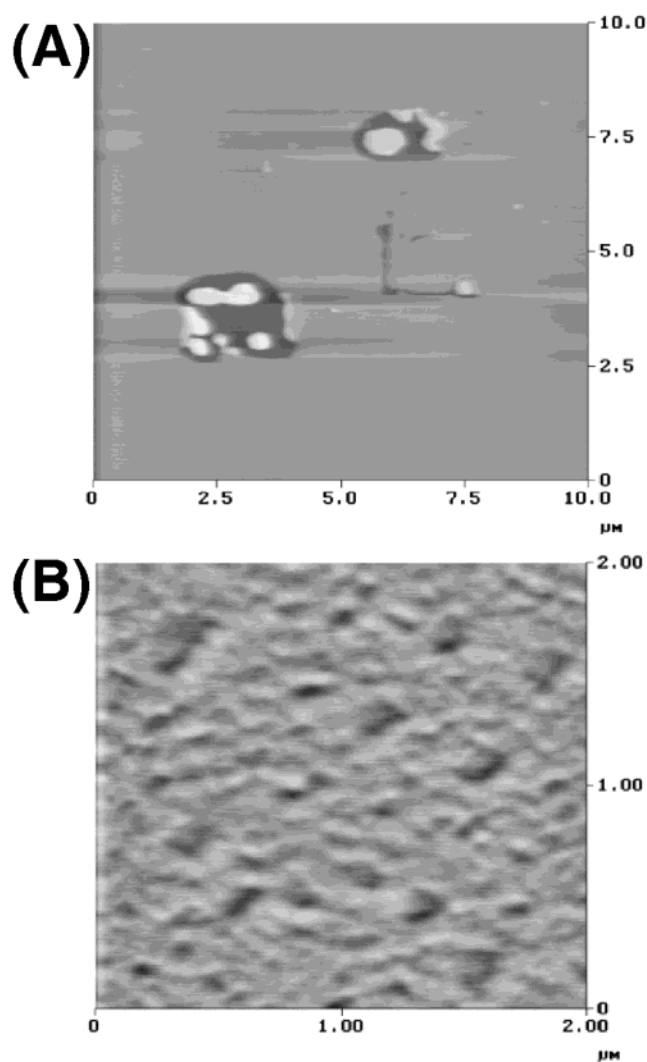


**Figure 4.** AFM images of (A) an untreated film and (B) a  $H^+$ -treated film.

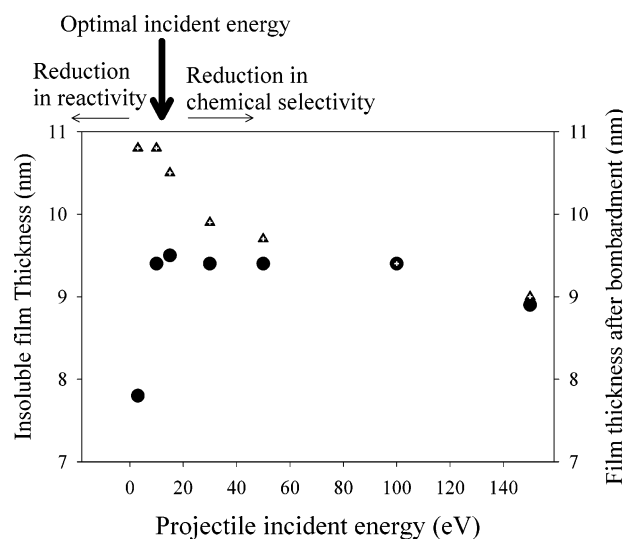


**Figure 5.** Extents of cross-linking (insoluble film thickness after solvent immersion, denoted as circles) and C–C cleavage (film thickness before solvent immersion, denoted as triangles) as a function of the projectile incident energy of  $H^+$  ion bombardment of an 11 nm dotriacontane film with a constant ion fluence of  $2 \times 10^{16}/\text{cm}^2$ .

the bombardment and gives the combined effects of film densification, physical sputtering, and collision-induced C–C

cleavage followed by fragment desorption. It increases rapidly when the ion energy is raised above 15 eV. On the other hand, the insoluble film thickness, which signifies cross-linking, was measured after the  $H^+$ -bombarded film was soaked in a solvent to dissolve any loose molecules. It reflects the desirable reactivity associated with the  $H^+$  collision, and was found to drop off quickly when the ion energy was reduced below 10 eV. The optimal collision energy was found to be about 10 eV. The presence of an optimal ion bombardment energy in the present reaction system convincingly validates the distinct nature of our proposed collision-induced route in comparison with the conventional hydrogen abstraction by atomic hydrogen carrying merely thermal energy. For ion bombardment below this optimal energy, the probability of collision-induced C–H cleavage drops and the resultant cross-linking reactivity is compromised. For ion bombardment with excessive energy, the probability of undesirable cleavage of bonds other than C–H rises and the chemical selectivity is lost.

The formation of a polymer film of 5–11 nm in thickness by  $H^+$  with an energy of less than 10 eV is intriguing as the direct projected range<sup>14</sup> should only be 0.5–1 nm. There are two possible mechanisms to increase the range of reaction in depth. First, interchain hydrogen hopping, which is generally referred to as chain transfer in polymer science,<sup>29</sup> can extend this range. For example, our quantum chemistry calculations using the Gaussian 98 package give a small energy barrier of 0.7 eV for hydrogen hopping to  $\text{CH}_3\text{CHCH}_2\text{CH}_3$  from a nearby  $\text{CH}_3\text{CH}_2\text{CH}_2\text{CH}_3$ , and the experimental value<sup>10</sup> of the  $\text{CH}_3/\text{C}_2\text{H}_6$  system is about 0.5 eV. Second, the scattered and recoiled hydrogens, due to the collision nature, should be highly agile in mobility in the hydrocarbon film until they are thermalized in the collision cascade.

To explore the applicability of the reaction design, we have repeated the experiments with a variety of organic molecule systems. For example, polymeric films with a single chemical functionality such as carboxylic acid were produced by cross-linking docosanoic acid molecules,  $\text{CH}_3(\text{CH}_2)_{20}\text{COOH}$ , with hyperthermal  $H^+$  at an ion fluence of less than  $1 \times 10^{16}/\text{cm}^2$ . In this reaction system, there is a small probability of CO–H bond cleavage and the subsequent formation of an ester or desorption of  $\text{CO}_2$ . The high population ratio of C–H to CO–H gives a forgiving tolerance in reaction parameters (proton energy and fluence) for achieving both high cross-linking reactivity and high chemical selectivity in the synthesis of a polymer film with a single functionality of carboxylic acid by cross-linking docosanoic acid molecules. To further scrutinize the chemical selectivity of the reaction design, we checked its applicability in cross-linking poly(acrylic acid) oligomers,  $\text{H}(\text{CH}_2\text{CHCOOH})_n\text{H}$  with an average  $n$  value of 30, which has a small C–H/CO–H ratio of 3. Although hyperthermal  $H^+$  collision can indeed convert a soluble poly(acrylic acid) film to an insoluble polymeric film, the optimization and control of reaction conditions for preserving the functionality of carboxylic acid were demandingly critical. To illustrate this process of engineering film functionality, we compare, in Figure 6, the XPS surface composition data of the virgin film prior to bombardment (sample A), the insoluble film after the 10 eV  $H^+$  collision at a fluence of  $5 \times 10^{15}/\text{cm}^2$  (sample B), the insoluble film formed at a fluence of  $2 \times 10^{16}/\text{cm}^2$  (sample C), and a poly(methyl

(29) Flory, P. J. *J. Am. Chem. Soc.* **1937**, *59*, 241–253.

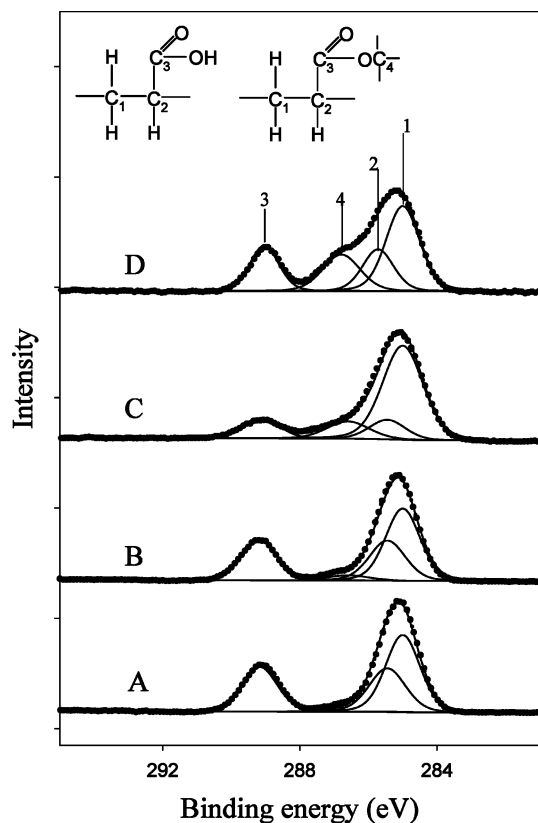


**Figure 6.** XPS C 1s spectra of (A) a virgin film of poly(acrylic acid), (B) a 10 eV  $H^+$  treated film at an ion fluence of  $5 \times 10^{15}/\text{cm}^2$ , (C) a 10 eV  $H^+$  treated film at an ion fluence of  $2 \times 10^{16}/\text{cm}^2$ , and (D) a virgin film of poly(methyl methacrylate) as a reference.

methacrylate) film (sample D), with the first and last as the respective references for carboxylic acid and ester functionalities. The fingerprint signature of an ester, a pair of C 1s peaks at  $C^3$  ( $\sim 289.2$  eV) and  $C^4$  ( $\sim 286.6$  eV) with an intensity ratio of 1:1, is inarguably different from that of carboxylic acid, which has  $C^3$  but no  $C^4$ . With this reference in hand, one can see clearly that sample B possesses carboxylic acid with little ester, whereas sample C possesses ester with nearly no carboxylic acid. The large reduction of the intensity of  $C^2$ ,  $C^3$ , and  $C^4$  relative to  $C^1$  in sample C further suggests that, in addition to the consumption in ester formation, some of the carboxylic acid units of the poly(acrylic acid) must have been lost in the collision process, possibly by the release of  $\text{CO}_2$ . The comparison of samples A–D demonstrates the feasibility in engineering film functionality with ion fluence, which is a common reaction attribute in most ion beam processes. Unsurprisingly, we also found that the suppression of ester formation and preservation of carboxylic acid can also be accomplished by reducing the proton energy below 6 eV, and that the reduction of ion energy increases the tolerance of ion fluence.

In another interesting set of trials, we found that, while the spatial range of cross-linking is about 10 nm from the collision site for saturated hydrocarbon as described earlier, this range extends to more than 1 mm when an unsaturated hydrocarbon such as polyisoprene ( $-\text{CH}_2\text{CH}=\text{CCH}_3\text{CH}_2-$ ) is used. In these trials, we spun-cast *trans*-polyisoprene molecules with an average molecular weight of 4,000,000 g/mol to a thickness of about 15 nm and further cross-linked them with 10 eV  $H^+$  passing through a shadow mask with a hole at the center. The collision-induced cross-linking made the processed film in-

soluble and increased the film's mechanical strength. Most intriguingly, these property changes were not confined to the unmasked area but were also observed in the masked area about 1.5 mm from the edge of the mask opening. This long-range reaction was not observed in all saturated organic molecules which we have tried. Our results show that chain transfer assisted by unsaturation can remarkably change the spatial range of cross-linking initiated by proton/hydrogen collision.

The results from these application trials confirm that collision-induced cross-linking adsorbed organic molecules with hyperthermal protons gives a new synthetic route for forming a polymer thin film with customized properties. The preferential C–H cleavage in this route overcomes the indiscriminating bond-breaking and thereby surface damage arising from irradiation by electrons, ions, and other energetic particles in most practical processes for thin film formation or surface modification which commonly employ gaseous plasmas. In our own previous studies of formation of dielectric films on semiconductors, we adopted the remote plasma technique by employing reactive neutrals in the downstream of a gaseous plasma source for dielectric film deposition to reduce the probability of undesirable bond-breakage of the semiconductor surface.<sup>30</sup> Similarly, in polymer science and technology, the methodology of “cross-linking with activated species of inert gases” (CASING) has been developed, also to minimize undesirable surface bond-breakage.<sup>31</sup> In CASING, excited argon or helium atoms are generated from a plasma and transported to the reaction site where they react with the substrate surface or gaseous molecules above the surface via Penning or resonance electronic energy transfer to cleave bonds in a controlled manner for initiating the required polymer reaction. Evidently, CASING is an established methodology with a wide scope of applicability.<sup>31</sup> In comparison, our hyperthermal proton approach is a novel route with chemical reactivity and selectivity uniquely related to the collisional and kinematic nature of the reaction design which is tunable by the proton energy and fluence. Admittedly the scope of applicability is narrower because the reactivity and selectivity both rest on the nature of hydrogen–hydrogen collision and the chemistry of hydrogen in the adsorbed molecules. Nevertheless, the scope is wide enough because there are so many precursor molecules having C–H bonds and appropriate chemical functionalities, molecules which can be cross-linked with hyperthermal protons for the production of polymeric films with practical industrial applications.

## Conclusion

We have extended the chemistry with a hammer approach in designing chemical reactions with kinematics considerations, by using the lightest chemical species (hydrogen ion) as a projectile with a few electronvolts in kinetic energy to cleave C–H bonds in adsorbed/condensed organic molecules and thereby induce their cross-linking. The degree of cross-linking is controlled by ion energy and fluence, and the original molecular chain and chemical functionalities can be well preserved during ion bombardment. The applications of the

- (30) Kwok, R. W. M.; Huang, L. J.; Lau, W. M.; Kasrai, M.; Feng, X.; Tan, K.; Ingrey, S.; Landheer, D. *J. Vac. Sci. Technol., A* **1994**, *12*, 2701–2704.
- (31) (a) Schonhorn, H.; Hansen, R. H. *J. Appl. Polym. Sci.* **1967**, *11*, 1416–1474. (b) Yu, Q. S.; Krentsel, E.; Yasuda, H. K. *J. Polym. Sci., Part A: Polym. Chem.* **1998**, *36*, 1583–1592. (c) Yasuda, H. K.; Lin, Y. S.; Yu, Q. S. *Prog. Org. Coat.* **2001**, *42*, 236–243.

method are demonstrated by the production of two-dimensional coherent and rigid polymer films having tailor-made chemical functionalities. Finally, this novel reaction design can be scaled up by employing a typical electron cyclotron resonance microwave plasma to generate hyperthermal  $H^+$  with a high flux in a large area. The process can be exploited in the production of polymeric optoelectronics<sup>32</sup> and other devices requiring ultrathin polymer films<sup>33</sup> with tailor-made chemical functionalities.

- (32) Ho, P. K. H.; Kim, J. S.; Burroughes, J. H.; Becker, H.; Li, S. F. Y.; Brown, T. M.; Cacialli, F.; Friend, R. H. *Nature* **2000**, *404*, 481–484.  
(33) Frank, C. W.; Rao, V.; Despotopoulou, M. M.; Pease, R. F. W.; Hinsberg, W. D.; Miller, R. D.; Rabolt, J. F. *Science* **1996**, *273*, 912–915.

**Acknowledgment.** We thank Professors Dennis Jacob and Z. F. Liu for their scientific inputs and advice, and Mr. W. L. Yim for his assistance in setting up the molecular dynamics simulation. This work was supported by the Research Grants Council, Hong Kong Special Administration Region, Grant Reference No. CUHK4106/98P.

**Supporting Information Available:** Detailed methods and additional XPS characterization results (PDF). This material is available free of charge via the Internet at <http://pubs.acs.org>.

JA046841D